Supplementary information for:

An ATP-dependent partner switch links flagellar C-ring assembly with gene expression

Vitan Blagotinsek[1,7], Meike Schwan[2,7], Wieland Steinchen[1], Devid Mrusek[1], John Hook[2], Florian Rossmann[2,6], Sven A. Freibert[3], Hanna Kratzat[4], Guillaume Murat[5], Dieter Kressler[5], Roland Beckmann[4], Morgan Beeby[6], Kai Thormann[2]* and Gert Bange[1]*

[1]Philipps-University Marburg, SYNMIKRO Research Center and Department of Chemistry, Hans-Meerwein-Strasse, 35043 Marburg, Germany

[2]Justus-Liebig-Universität, Department of Microbiology and Molecular Biology, Heinrich-Buff-Ring 26, 35392 Giessen, Germany

[3]Philipps-Universität Marburg, Institut für Zytobiologie und Zytopathologie Robert-Koch-Str. 6, 35032 Marburg, Germany

[4]Ludwig-Maximilians-Universität, Genzentrum and Department of Biochemistry, Feodor-Lynen-Straße 25, 81377 Munich, Germany

[5]University of Fribourg, Department of Biology, Chemin du Musée 10, CH-1700, Fribourg, Switzerland

[6]Imperial College London, Department of Life Sciences, South Kensington Campus, London SW7 2AZ, UK. ORCID: 0000-0001-6413-9835

[7]These authors contribute equally to this work.

*Correspondence: gert.bange@synmikro.uni-marburg.de; Kai.Thormann@mikro.bio.uni-giessen.de

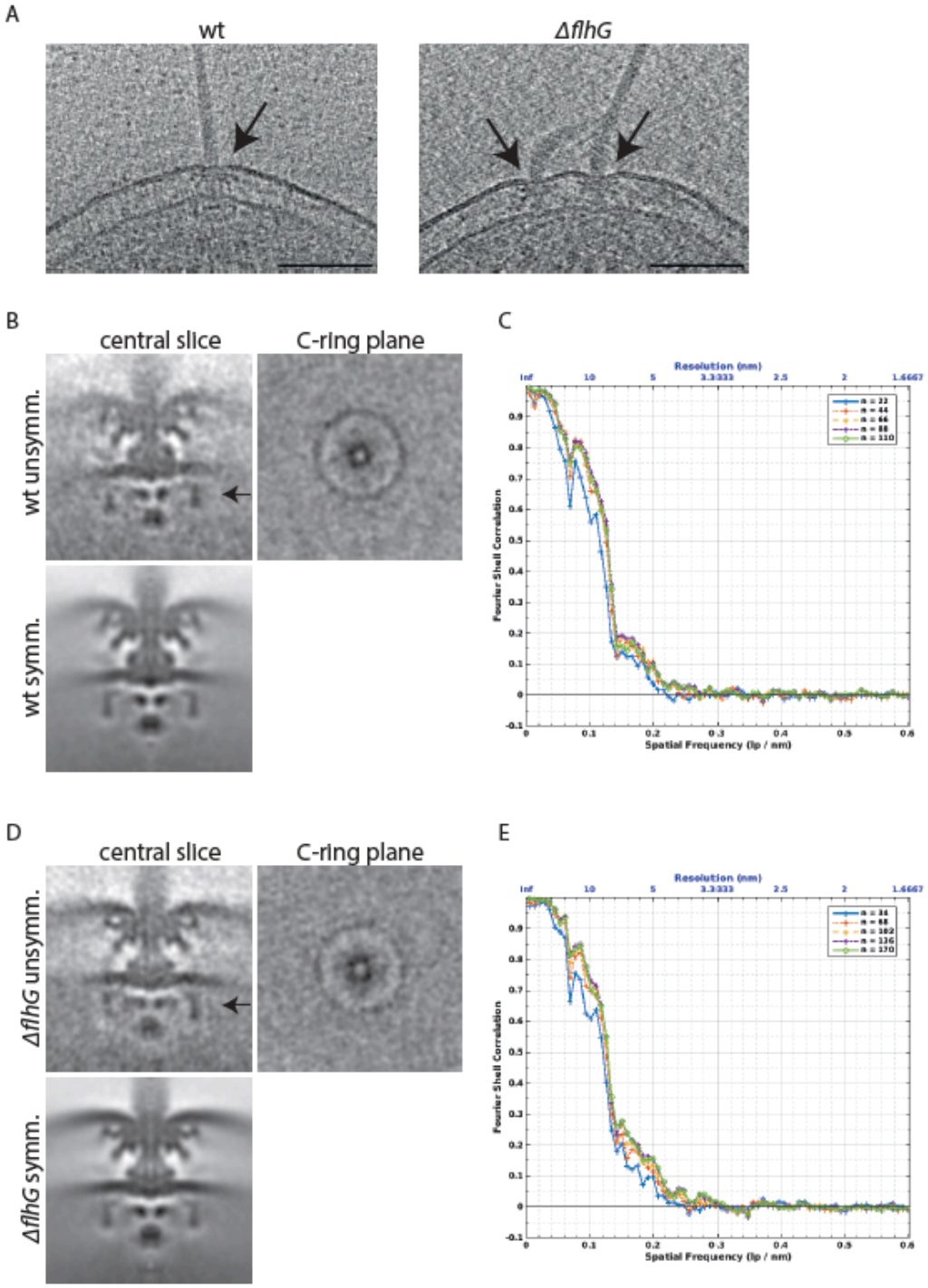

Supplementary Fig. S1: Cryo-electron tomography of *S. putrefaciens* flagella in the presence and absence of FlhG. (a) Slices through tomograms showing flagellated cell poles from *S. putrefaciens* wildtype and *flhG* deletion strain with arrows pointing at flagellar motors. Scale bar represents 100 nm. **(b & d)** 100 nm x 100 nm slices through subtomogram averages of the *S. putrefaciens* wiltype **(b)** and Δ*flhG* motor **(d)**. Top panels show the unsymmetrised structures as horizontal slices in the C-ring plane (right) indicated by arrows in the vertical central slices (left). Bottom panels show the

central slices of the motor structures with applied C100 symmetry. **(c & e)** FSC (Fourier Shell Correlation) curves of the *S. putrefaciens* wiltype **(c)** and Δ*flhG* motor **(e)**. Resolution at a 0.5 threshold of both unsymmetrised motor structures is approximately 7.8 nm.

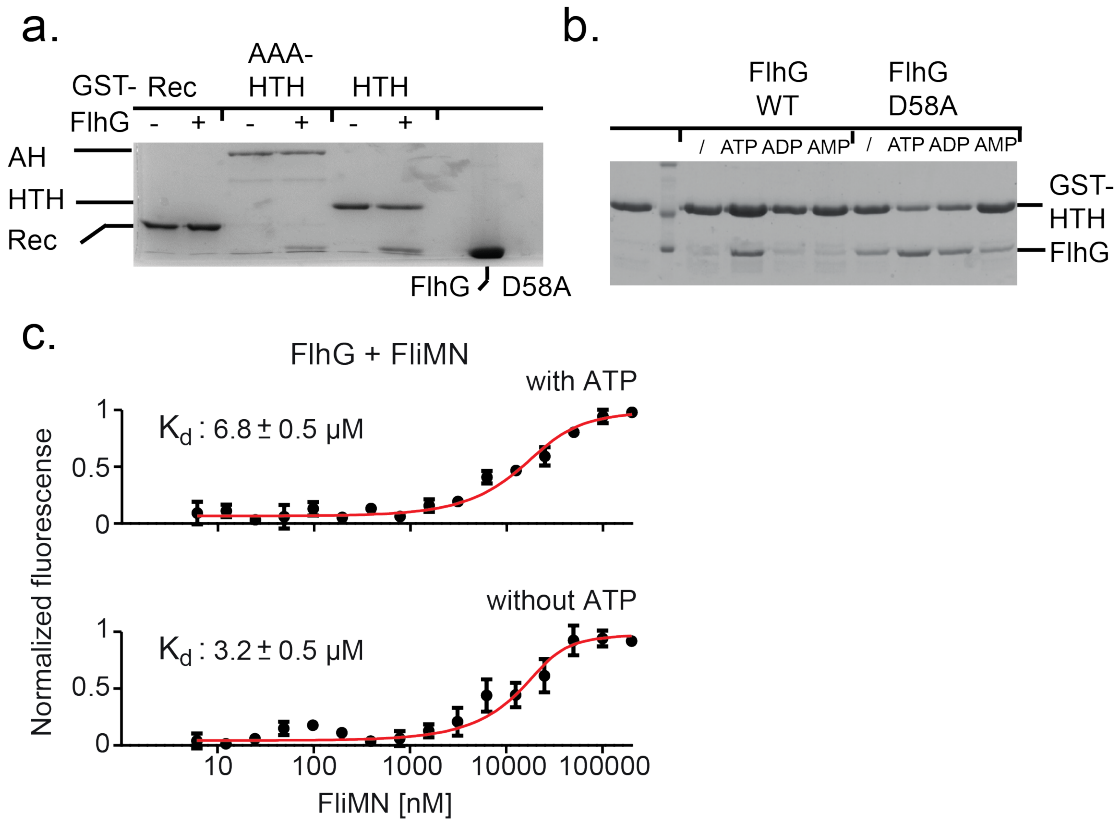

Supplementary Fig. S2: Nucleotide dependence of FlrA-HTH and FliMN interactions with FlhG. (a) Pulldown assay probing the interaction of FlrA truncations with the FlhG D58A variant in absence of ATP. **(b)** Pulldown assay probing the interaction of FlrA-HTH with native FlhG or the D58A variant. Nucleotides were present at final concentrations of 0.25 mM. **(c)** Interaction of FlhG with FliMN probed by microscale thermophoresis in presence of 0.25 mM ATP (upper panel) or without ATP (lower panel). Data represent mean ± SD of n = 3 technical replicates.

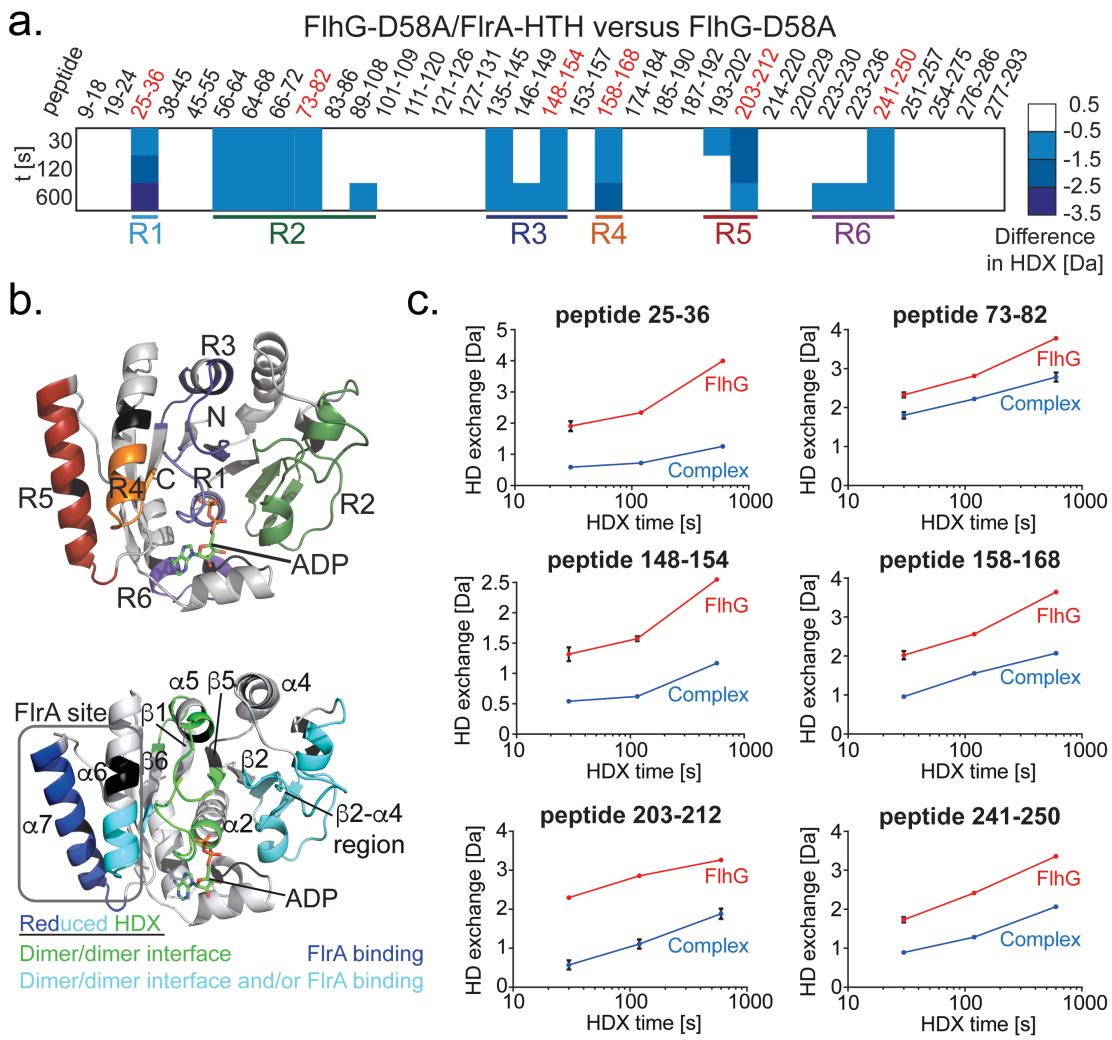

Supplementary Fig. S3. HDX-MS of the FlhG/FlrA-HTH interaction. (a) Representative peptides of $FlhG_{D58A}$ are coloured according to their difference in HDX between the $FlhG_{D58A}$/FlrA-HTH complex and $FlhG_{D58A}$ alone. **(b)** Areas of $FlhG_{D58A}$ exhibiting differences in HDX in a structural model of FlhG (generated with Swissmodel based on the structure of homodimeric FlhG from *Geobacillus thermodenitrificans*; PDB-ID 4RZ3; (1)). Colouring is based on the location of the six regions (top) or on the implication of peptides with decreased HDX in establishing the homodimeric interface of FlhG (green), interface establishment and/or FlrA binding (cyan) or FlrA binding (blue) alone (bottom). **(c)** Hydrogen/deuterium (HD) exchange profiles of representative $FlhG_{D58A}$ peptides (colored red in panel a) in the $FlhG_{D58A}$/FlrA-HTH complex (blue) and $FlhG_{D58A}$ alone (red). Data represent the mean ± SD of three technical replicates.

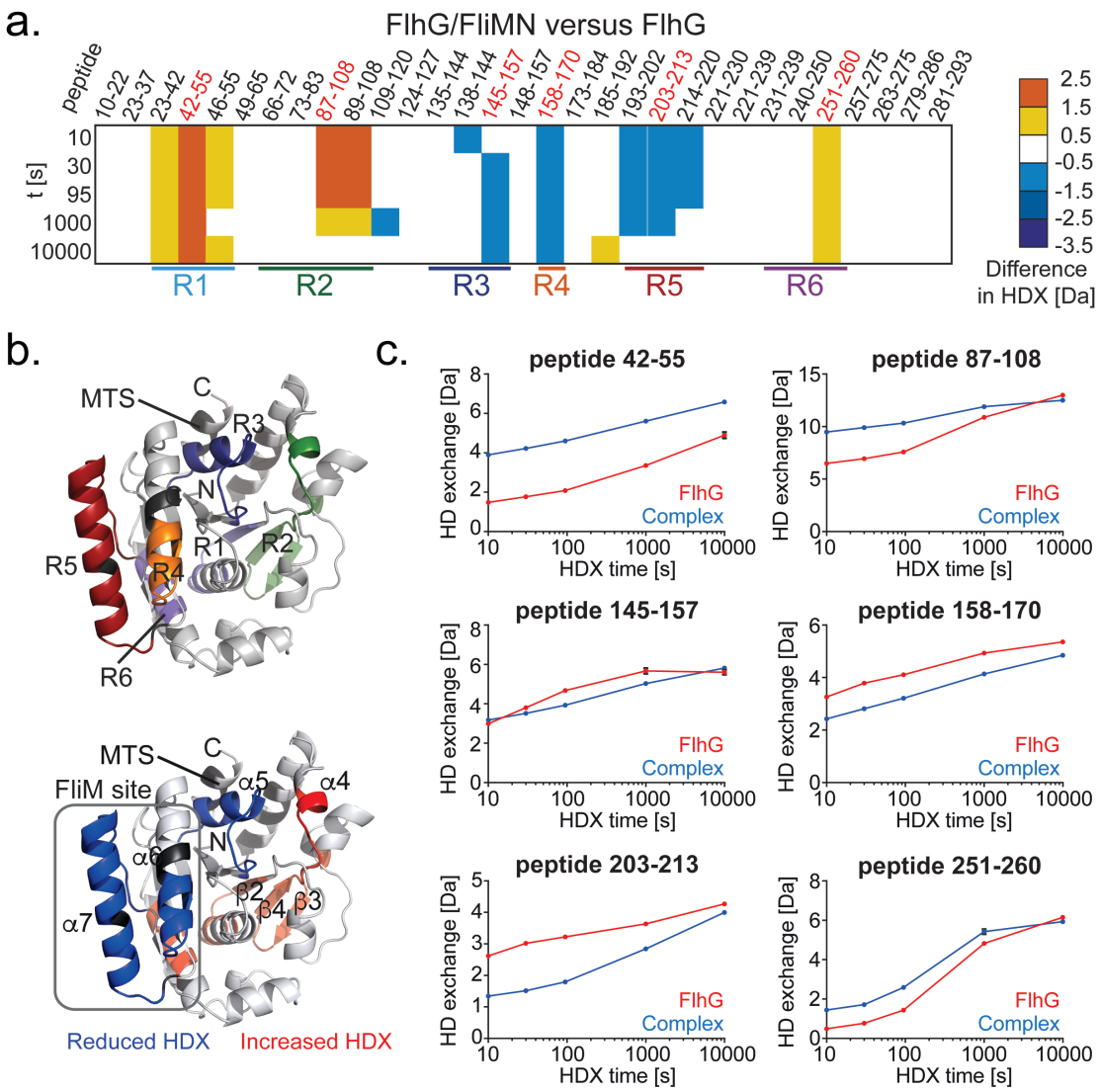

Supplementary Fig. S4: HDX-MS of the interaction of FlhG with FliMN. (a) Representative peptides of FlhG are coloured according to their difference in HDX between the FlhG/FliMN complex and FlhG alone. **(b)** Areas of FlhG exhibiting differences in HDX in a structural model of FlhG (generated with Swissmodel based on the structure of monomeric FlhG from *Geobacillus thermodenitrificans*; PDB-ID 4RZ2; (1). Colouring is based on the location of the six regions (top) or reduced/increased HDX of FlhG in context of the FlhG/FliMN complex (bottom). **(c)** Hydrogen/deuterium (HD) exchange profiles of representative FlhG peptides (colored red in panel a) in the FlhG/FliMN complex (blue) and FlhG alone (red). Data represent the mean ± SD of three technical replicates.

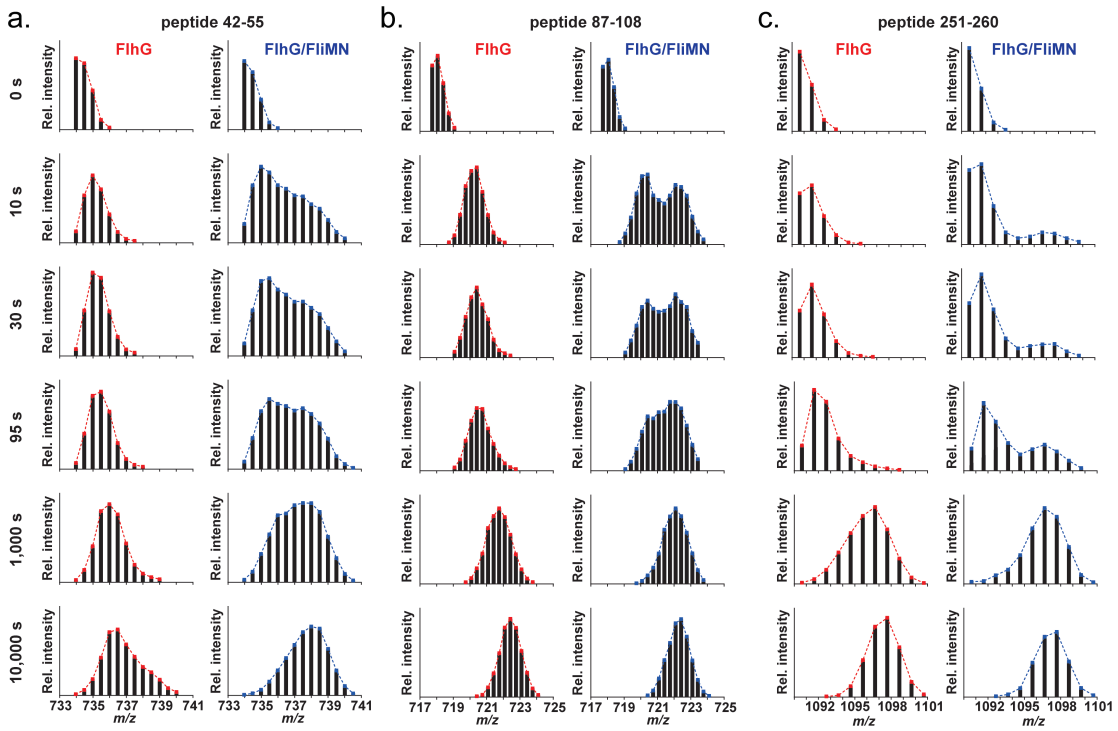

Supplementary Fig. S5: Bimodality of FlhG in the FlhG/FliMN complex. (a-c) Mass spectra of representative peptides 42-55 (**a**), 87-108 (**b**) and 251-260 (**c**) of FlhG that exhibit bimodal behavior in the FlhG/FliMN complex. The occurrence of a fast-exchanging population is indicative for unfolding of secondary structures rendering the amide protons more accessible for HDX.

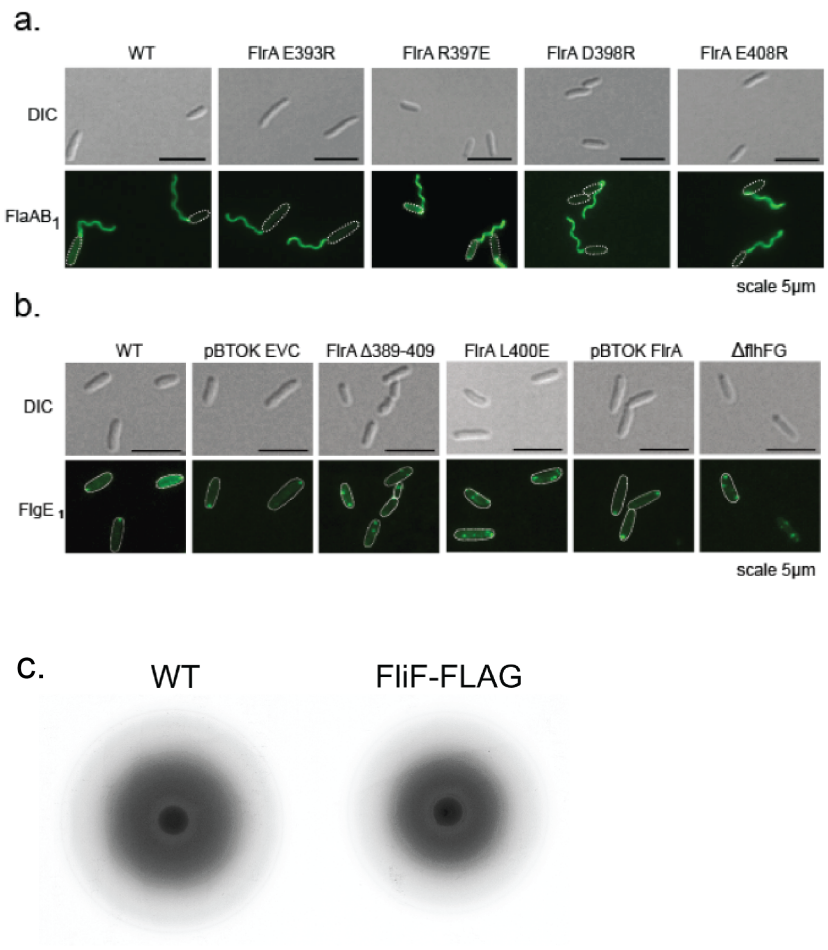

Supplementary Fig. S6: Hook and filament stains of different FlrA mutants. (a) AlexaFluor maleimide 488 stains and DIC images of flagellar filaments in *S. putrefaciens CN-32* WT and mutant strains with WT-like phenotypes. The scale bar equals 5 µm. **(b)** AlexaFluor maleimide 488 stains and DIC images of flagellar hooks corresponding to stains of flagellar filaments in Fig. 4a. **(c)** Motility of wildtype *S. putrefaciens* strain and a strain producing a N-terminally FLAG-tagged FliF.

Table 1: Bacterial strains

Identifier	Relevant genotype or description	Source
Escherichia coli		
DH5α λpir	φ80d*lacZ* ΔM15 Δ(*lacZYA-argF*)U169 *recA1 hsdR17 deoR thi-l supE44 gyrA96 relA1*/λpir	(2)
WM3064	*thrB1004 pro thi rpsL hsdS lacZ* ΔM15 RP4-1360 Δ(*araBAD*) 567Δ*dapA* 1341::[*erm pir*(wt)]	W. Metcalf, University of Illinois, Urbana-Champaign
Shewanella putrefaciens		
S271	CN-32, wildtype	(3)
S3133	Δ*flhG*, ΔSputcn32_2560, markerless deletion of *flhG*	(1)
S4162	FliM-mCherry/Δ*flhG*/FlhG-GFP; Sputcn32_2569 Sputcn32_2560; markerless insertion of *fliM* with a C-terminal mCherry-tag, markerless in frame deletion of *flhG* and stable integration of overproduction vector pBTOK producing full length protein FlhG with a C-terminal sfGFP-tag	This study
S4163	$FliM_{\Delta N}$-mCherry/Δ*flhG*/FlhG-GFP; Sputcn32_2569 Sputcn32_2560; markerless insertion of *fliM*with deletion of residues 2-28 with a C-terminal mCherry-tag, markerless in frame deletion of *flhG* and stable integration of overproduction vector pBTOK producing full length protein FlhG with a C-terminal sfGFP-tag	This study
S3783	pBTOK EVC, stable integration of overproduction vector pBTOK as empty vector control in wildtype background	(4)
S5917	pBTOK FlhG, pBTOK-Sputcn32_2560; stable integration of overproduction vector pBTOK producing the full length protein FlhG	This study
S4401	$FlaAB_{cys}$; $Sputcn32\_2586_{T174C}$ $Sputcn32\_2585_{T166C}$ ΔSputcn32_3456 ΔSputcn32_3455; markerless insertion of cysteine-labeled *flaA* gene into *ΔflaA* and cysteine-labeled *flaB* gene into *ΔflaB* and deletion of lateral flagellin genes $flaA_2$ and $flaB_2$	(5)
S5910	$flgE_{T183C}$; Sputcn32_2594-T183C ΔSputcn32_3444 - Sputcn32_3485; markerless insertion of cysteine-labeled *flgE* gene into Δ*flgE* and in frame deletion of lateral flagella gene cluster	This study
S6000	*ΔflrA*in strain S4401; ΔSputcn32_2580; markerless in frame deletion of *flrA* in $FlaAB_{-cys}$ $\Delta flaAB_2$ (S4401) background	This study
S6021	$FlrA_{\Delta 389-409}$ in strain S6000; $\Delta Sputcn32\_2580_{389-409}$; markerless insertion of $flrA_{\Delta 389-409}$ in $FlaAB_{-cys}$ *ΔflrA* $\Delta flaAB_2$ (S6000) background	This study
S4964	*ΔflhG* in strain S4401; ΔSputcn32_2560; markerless in frame deletion of *flhG* in $FlaAB_{-cys}$ $\Delta flaAB_2$ (S4401) background	This study
S5984	$FlhG_{K175E}$ in strain S4964; $Sputcn32\_2560_{K175E}$; markerless insertion of $flhG_{K175E}$ in $FlaAB_{-cys}$ *ΔflhG* $\Delta flaAB_2$ (S4964) background	This study
S6116	$FlhG_{D58A}$ in strain S4964; $Sputcn32\_2560_{D58A}$; markerless insertion of $flhG_{D58A}$ in $FlaAB_{-cys}$ *ΔflhG* $\Delta flaAB_2$ (S4964) background	This study
S6782	$FlhG_{D58A\ K175E}$ in strain S4964; $Sputcn32\_2560_{D58A\ K175E}$; markerless insertion of $flhG_{D58A\ K175E}$ in $FlaAB_{-cys}$ *ΔflhG* $\Delta flaAB_2$ (S4964) background	This study

S6054	*ΔflhFG* in strain S4401; ΔSputcn32_2561 ΔSputcn32_2560; markerless in frame deletion of *flhFG* in FlaAB$_{\text{-cys}}$ *ΔflaAB$_2$* (S4401) background	This study
S6103	pBTOK FlrA-FLAG in strain S4401; Sputcn32_2580; stable integration of overproduction vector pBTOK producing the full length protein FlrA with a C-terminal FLAG-tag in FlaAB$_{\text{-cys}}$ *ΔflaAB$_2$* (S4401) background	This study
S6730	pBTOK FlhG in strain S4401; Sputcn32_2560; stable integration of overproduction vector pBTOK producing the full length protein FlhG in FlaAB$_{\text{-cys}}$ *ΔflaAB$_2$* (S4401) background	This study
S6586	pBTOK EVC in strain S4401; stable integration of overproduction vector pBTOK as empty vector control in the FlaAB$_{\text{-cys}}$ *ΔflaAB$_2$* (S4401) background	This study
S6180	*ΔflrA* in strain S5910; ΔSputcn32_2580; markerless in frame deletion of *flrA* in the FlgE-cys *ΔflaAB$_2$* (S5910) background	This study
S6188	FlrA$_{\Delta 389\text{-}409}$ in strain S6180 background; ΔSputcn32_2580$_{\Delta 389\text{-}409}$; markerless insertion of *flrA* with deletion of residues 389-409 in the FlgE$_{\text{-cys}}$ *ΔflaAB$_2$* (S5910) background	This study
S6216	*ΔflhFG* in strain S5910; ΔSputcn32_2561 ΔSputcn32_2560; markerless in frame deletion of *flhFG* in FlgE-cys *ΔflaAB$_2$* (S5910) background	This study
S6207	pBTOK FlrA-FLAG in strain S5910; Sputcn32_2580; stable integration of overproduction vector pBTOK producing the full length protein FlrA with a C-terminal 3xFLAG-tag in FlgE$_{\text{-cys}}$ *ΔflaAB$_2$* (S5910) background	This study
S6206	pBTOK EVC in strain S5910; stable integration of overproduction vector pBTOK as empty vector control in FlgE$_{\text{-cys}}$ *ΔflaAB$_2$* (S5910) background	This study
S6570	FlrA$_{L400E}$ in strain S6000; Sputcn32_2580$_{L400E}$; markerless insertion of *flrA$_{L400E}$* in FlaAB$_{\text{-cys}}$ *ΔflrA ΔflaAB$_2$* (S6000) background	This study
S6571	FlrA$_{L400E}$ in strain S6180; Sputcn32_2580$_{L400E}$; markerless insertion of *flrA$_{L400E}$* in FlgE$_{\text{-cys}}$ *ΔflrA ΔflaAB$_2$* (S6180) background	This study
S4175	FlrA-FLAG; Sputcn32_2580; markerless insertion of *flrA* with a C-terminal 3xFLAG-tag	This study
S6149	FlrA$_{\Delta 389\text{-}409}$-FLAG; Sputcn32_2580$_{\Delta 389\text{-}409}$; markerless insertion of *flrA* with deletion of residues 389-409 with a C-terminal FLAG-tag	This study
S6586	pBTOK FlhFG in strain S4401; ΔSputcn32_2561 Sputcn32_2560; stable integration of overproduction vector pBTOK producing the full length protein FlhF and FlhG in FlaAB$_{\text{-cys}}$ *ΔflaAB$_2$* (S4401) background	This study
S6730	pBTOK EVC in strain S6570; stable integration of overproduction vector pBTOK as empty vector control in FlaAB$_{\text{-cys}}$ *ΔflaAB$_2$ flrA$_{L400E}$* (S6570) background	This study
S6732	pBTOK FlhG in strain S6570; Sputcn32_2560; stable integration of overproduction vector pBTOK producing the full length protein FlhG in FlaAB$_{\text{-cys}}$ *ΔflaAB$_2$ flrA$_{L400E}$* (S6570) background	This study
S4192	FlrA-FLAG FliM-FLAG FlhG-FLAG; Sputcn32_2580 Sputcn32_2569 Sputcn32_2560; markerless insertion of *flrA* with a C-terminal 3xFLAG-tag, *fliM* with a C-terminal 3xFLAG-tag and *flhG* with a C-terminal 3xFLAG-tag	This study
S6564	FlrA$_{E393R}$ in strain S6000; Sputcn32_2580$_{E393R}$; markerless insertion of *flrA$_{E393R}$* in FlaAB$_{\text{-cys}}$ Δ*flrA* Δ*flaAB$_2$* (S6000) background	This study
S6566	FlrA$_{R397E}$ in strain S6000; Sputcn32_2580$_{E393R}$; markerless insertion of *flrA$_{R397E}$* in FlaAB$_{\text{-cys}}$ Δ*flrA* Δ*flaAB$_2$* (S6000) background	This study

S6568	FlrA$_{D398R}$ in strain S6000; Sputcn32_2580$_{E393R}$; markerless insertion of *flrA*$_{D398R}$ in FlaAB$_{cys}$ Δ*flrA* Δ*flaAB*$_2$ (S6000) background	This study
S6572	FlrA$_{E408R}$ in strain S6000; Sputcn32_2580$_{E393R}$; markerless insertion of *flrA*$_{E393R}$ in FlaAB$_{cys}$ Δ*flrA* Δ*flaAB*$_2$ (S6000) background	This study
S4295	FliF-FLAG; Sputcn32_2576; markerless insertion of *fliF* with a N-terminal 3xFLAG-tag in a wildtype (S271) background	This study
S4296	FliF-FLAG Δ*flrA*; Sputcn32_2576 Sputcn32_2580; markerless deletion of flrA in FliF-FLAG (S4295) background	This study
S6046	FliF-FLAG FlrA$_{L400E}$; Sputcn32_2576 Sputcn32_2580$_{L400E}$; markerless insertion of *flrA*$_{L400E}$ in FliF-FLAG Δ*flrA* (S4296) background	This study
S6886	FliF-FLAG pBTOK EVC; Sputcn32_2576; stable integration of overproduction vector pBTOK as empty vector control in FliF-FLAG (S4295) background	This study
S6887	FliF-FLAG pBTOK FlhG; Sputcn32_2576 Sputcn32_2560; stable integration of overproduction vector pBTOK producing the full length protein FlhG in FliF-FLAG (S4295) background	This study

Supplementary References.

1. Schuhmacher JS, *et al.* (2015) MinD-like ATPase FlhG effects location and number of bacterial flagella during C-ring assembly. *Proc Natl Acad Sci U S A* 112(10):3092-3097.
2. Miller VL & Mekalanos JJ (1988) A novel suicide vector and its use in construction of insertion mutations: osmoregulation of outer membrane proteins and virulence determinants in Vibrio cholerae requires toxR. *J Bacteriol* 170(6):2575-2583.
3. James K. Fredrickson JMZ, David W. Kennedy, Hailang Dong, Tullis C. Onstott, Nancy W. Hinman, Shu-mei Li (1998) Biogenic iron mineralization accompanying the dissimilatory reduction of hydrous ferric oxide by a groundwater bacterium. *Geochimica et Cosmochimica Acta* 62(19-20):3239-3257.
4. Rossmann F, *et al.* (2015) The role of FlhF and HubP as polar landmark proteins in Shewanella putrefaciens CN-32. *Mol Microbiol* 98(4):727-742.
5. Kuhn MJ, Schmidt FK, Eckhardt B, & Thormann KM (2017) Bacteria exploit a polymorphic instability of the flagellar filament to escape from traps. *Proc Natl Acad Sci U S A* 114(24):6340-6345.